Predictive-TOPSIS-based MPPT for PEMFC Featuring Switching Frequency Reduction

Jye Yun Fam[1], Shen Yuong Wong[2], Mohammad Omar Abdullah[3], Kasumawati Lias[4], Saad Mekhilef[5], Hazrul Mohamed Basri[6]

[1,3,4,6]Faculty of Engineering, Universiti Malaysia Sarawak, 94300 Kota Samarahan, Sarawak, Malaysia
[2]Department of Electrical and Electronics Engineering, Xiamen University Malaysia, Sepang 43900, Malaysia
[5]School of Science, Computing and Engineering Technologies, Swinburne University of Technology, Hawthorn, Melbourne, VIC 3122, Australia

Article Info	ABSTRACT
	A maximum power point tracking (MPPT) for a proton exchange membrane fuel cell (PEMFC) using a combination of conventional finite control set model predictive control (FCS-MPC) and Technique for Order of Preference by Similarity to Ideal Solution (TOPSIS) is proposed in this paper. The key idea is to maximize the power generation from a PEMFC while minimizing the switching frequency of the power converter. The FCS-MPC technique is formulated to track the maximum power of PEMFC highly affected by ever-changing internal parameters. Meanwhile, the TOPSIS algorithm is applied to overcome the potential weaknesses of insulated-gate bipolar transistor (IGBT), which can only withstand a lower switching frequency. In this project, all simulations were run using MATLAB software to display the output power of the PEMFC system. As a result, the proposed predictive-TOPSIS-based MPPT algorithm can track the MPP for various PEMFC parameters within 0.019 s with an excellent accuracy up to 99.11%. The proposed MPPT technique has fast-tracking of the MPP locus, excellent accuracy, and robustness to environmental changes.

Corresponding Author:

Shen Yuong Wong,
Department of Electrical and Electronics Engineering,
Xiamen University Malaysia,
Sepang 43900, Malaysia.
Email: shenyuong.wong@xmu.edu.my

1. INTRODUCTION

Renewable energy sources (RESs) are used to replace fossil fuels in various technical applications because the Earth suffers fossil fuel depletion [1]. Thus, finding storage devices with RESs is critical to avoid the energy shortfall while maintaining sufficient power to load. The fuel cell (FC) is an electrochemical device converting chemical reaction-free energy into electrical energy. It is one of the most important types of electrical energy storage systems. In FC power generation process, the by-products are only water and heat, while hydrogen and air are sources. It has a high-power efficiency of up to 45%, remarkably higher than the other traditional energy generators [2]. It is known for its exceptional reliability, ease of installation, and low fuel consumption. Its advantages also include high efficiency, low environmental pollution, and it is not location specific. FC has a wide range of uses due to its power modularity ranging from a few kilowatt to megawatt scale. [3]. This technology is used in various locations, including residential, commercial, and industrial.

One of the most prevalent types of FC is the proton exchange membrane fuel cell (PEMFC) because of their solid electrolyte, quick startup, and low operating temperature [4]. The behavior of the PEMFC heavily depends on its operating conditions, including partial pressures of reactance gases, membrane water content, and temperature. Although the PEMFCs have high efficiency, the power extracted from them is not always the

maximum power due to the ever-changing internal parameter of PEMFC. PEMFC power is characterizable by a nonlinear polarization curve. Different polarization curves populate a unique point where the maximum power occurs, and this point is termed as maximum power point (MPP). A maximum power point tracking (MPPT) technique is necessary to reach the PEMFC's optimal operating point.

In a PEMFC power system, an MPPT controller must obtain a high output power from the FC. Based on the PEMFC mathematical model, any FC parameters, such as operating temperature, partial pressure of reactant gases, and membrane water content, can highly affect its output power. For instance, Figure 1(a) and 1(b) depict the V–I and P–I polarization curves of PEMFC, demonstrating that different PEMFC operating temperatures lead to varying MPP.
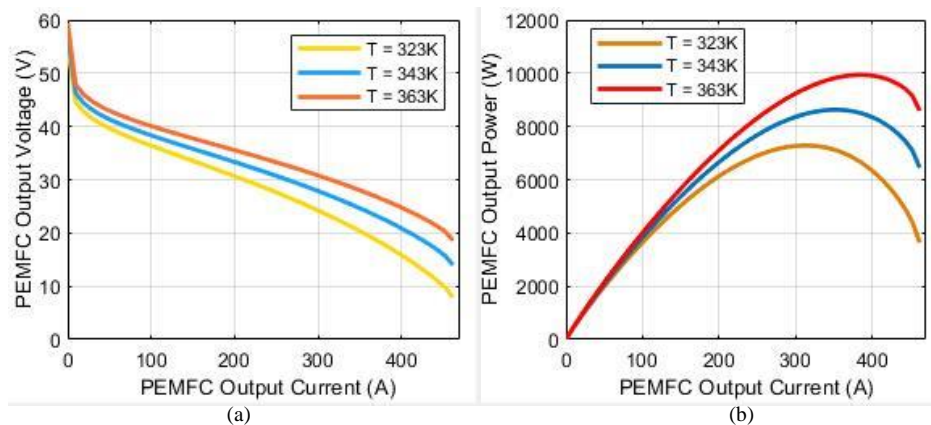

Figure 1. Polarization Curve of PEMFC for Different Operating Temperatures,
(a) V–I Polarization Curve, b) P–I Polarization Curve

In the past, various MPPT approaches existed in the literature. The common MPPT methods are Sliding Mode Control (SMC) [5], [6], Perturb and Observe (P&O) [7]–[9], and current estimation method [10], [11]. Advanced techniques include Fuzzy Logic Control (FLC) [12], Radial Basis Function Network (RBFN) [13], Particle Swarm Optimizer (PSO) [12], [14], and model predictive control (MPC) techniques [15]. Some techniques can be combined with the proportional-integral-derivative (PID) controller, making the performance more stable [14].

Jiao [5] and Abdi et al. [6] used the SMC MPPT on a FC power system. A DC–DC boost converter can be used to control the output voltage. By synthesizing a sliding surface, an adequate control law can be selected. The sliding function algorithm controls the duty cycle of the DC–DC converter and regulates the output voltage of the FC. The findings suggest that the SMC technique could maintain maximum output power and resist external variables.

Naseri et al. [7], Dharani [8], and Dargahi et al. [9] presented a P&O method in a PEMFC system. The P&O approach compares the changing of current and power at each sampling instant to the step perturbation necessary to achieve maximum output power. This MPPT approach can extracts the FC power at the maximum power point.

Luta [12] proposed and compared the MPPT technique performance between PSO and FLC for FC stacks. Both techniques can regulate the PEMFC output voltage to the voltage at MPP and extract the maximum power from the FC. The FLC approach uses the "Center of Gravity" of defuzzification to identify the crisp output, which includes a fuzzy set as a rule. PSO conceptualizes a group particles having the same goal. These particles represent some potential solutions with a certain effort to find the best solution. The movement of the particles is then updated based on the past leading position until the optimum solution is found. The results show that the PSO method outstands the FLC method because it is quicker to track the MPP, and it has a lower power overshoot. However, FLC had better performance on settling time and lower power undershoot.

Using a PID controller, Ahmadi et al. [14] enhanced the PSO technique on the FC system. Three parameters are required in the PID controller: proportional gain, integral gain, and derivative gain. During the operation, the PID controller will first receive the data from the PSO algorithm as the reference voltage. Then, the FC voltage is regulated to approach the reference voltage. The PSO–PID method is compared with SMC and P&O approaches. From the results, the PSO–PID method shows excellent performance than P&O and SMC methods. It has low power fluctuations, excellent accuracy, and quick time response under variable PEMFC parameters.

Srinivasan et al. [13] also developed an artificial neural network MPPT controller for PEMFC using the RBFN technique. The RBFN is divided into three layers: input, hidden layer, and output. The RBFN

controller receives the voltage and current of the PEMFC as inputs, the nonlinear radial basis activation function as the hidden layer, and the duty cycle of the power converter as the output for the FC system. The greatest power achieved from the PEMFC was compared using the conventional DC–DC boost, quadratic DC–DC boost, and reconfigured quadratic DC–DC boost converters. The RBFN-based MPPT approaches were also compared with P&O and FLC techniques. The simulation results show that the MPPT by RBFN has the highest accuracy on tracking the MPP, and the reconfigured quadratic DC–DC boost converter excellently performs on DC power dissipation.

MPC offers the benefit of predicting the behavior of the variables in a system. The controller then calculates the superior actuation based on a set of optimization criteria [16]. Derbeli et al. [15] presented a high-performance output current control for PEMFC using the MPC technique. This proposed technique is only a stable performance tracking method but not an MPPT. It forecasts the next two sampling steps output current of the PEMFC and is compared to a constant reference current. Then, the cost function is calculated based on the output and reference currents. The switching combination with the lowest cost function value will be selected. The findings reveal that the MPC approach chooses the optimum switching state for every sampling state. Although this MPC technique does not involve an MPPT approach, it demonstrates that MPC's tracking mechanism kept the output current at the reference value.

Table 1. Comparison of MPPT Methods

MPPT Methods	Advantages	Disadvantages	Reference
Sliding Mode Control (SMC)	• Fast MPP tracking • High stability	• High complexity • High-power ripple • Low stability	[5], [6], [14]
Perturb and Observe (P&O)	• Low complexity	• Slow tracking of MPP • High-power ripple	[7]–[9]
Incremental Conductance (IC)	• Low complexity	• Slow tracking of MPP • Low stability	[1]
Radial Basis Function Network (RBFN)	• Fast MPP tracking	• High-power ripple • High complexity	[13]
Fuzzy Logic Control (FLC)	• Fast MPP tracking • High stability	• High complexity • High-power ripple	[12]
Particle Swarm Optimizer (PSO)	• Fast MPP tracking • High stability	• High-power ripple • High computational burden • High complexity	[12]
Particle Swarm Optimizer with Proportional-Integral-Derivative (PID)	• Fast MPP tracking • Low power ripple • High stability	• High computational burden • High complexity	[14]
Model Predictive Control	• High stability • Low complexity	• Slow tracking of MPP	[15]

To generate a high-power efficiency conversion, the switching frequency of the DC–DC converter becomes an important proportion. This is because the switching losses are decreased after the switching frequency reduction. The power losses of the switch in the power electronics module comprise switching and conduction losses [17]. Switching losses are associated with the intervals of switching ON or OFF. During the switching intervals, the voltage and current have a rising and falling waveform. Conduction losses occur during the conduction period of power electronics switching devices due to their resistance. Therefore, reducing the switching loss is important in power electronics, including decreasing thermal stress and increasing power efficiency [18].

Onederra et al. [18] presented a Variable Switching Frequency (VSF) technique in a three-phase voltage source inverter (VSI) to minimize the switching loss. Space Vector Pulse Width Modulation (SVPWM) algorithm was also applied to maintain the output current quality. In SVPWM, constant switching frequency was modified into VSF to reduce the switching loss. As a result, the VSF method minimizes the switching frequency, while the total harmonic distortion only shows a minor increment.

Cui et al. [19] also presented a switching frequency reduction-based model predictive direct power control technique for a power inverter. For a three-phase inverter, power quality is the priority. When the switching frequency reduction technique is included, a cost function is derived to consider the active power, reactive power, and the switching frequency reduction with a constant coefficient. By minimizing the cost function, the optimal switching states can be determined. Multicost functions with different coefficients were derived to overcome the contradiction between the power quality and the switching frequency. The results show that the multicost function can maintain high-power quality while minimizing the switching frequency and reducing the switching loss.

Oliveira et al. [20] designed two parallel Uninterruptible Power Supplies (UPS) subjected to a Zero Sequence Circulating Current, which will increase the power losses. To achieve maximum global system

efficiency, the switching frequency reduction technique is applied in two parallel UPS systems. The switching frequency of the grid- and load-side converters in the UPS systems are controlled by FCS-MPC. An optimal switching state will be chosen by minimizing the global converter cost function after predicting the system state. The efficiency of the system increases when the switching frequency is reduced.

Dang et al. [21] introduced a low switching frequency technique in time-based MPPT applied in a photovoltaic (PV) system. To track the MPP, switching frequency and capacitance turning were applied to obtain a large power range. Capacitance turning was used first through a capacitor bank. Then, the system slowly increases the switching frequency to track the MPP. When the MPP is tracked, the minimum switching frequency is used so that the switching loss is the minimum. The results show that the low switching frequency with the time-based MPPT method can track the MPP of the PV.

When this switching frequency reduction is applied in the MPPT technique, the output power fluctuation will also be increased. This phenomenon is proven by Lee et al. [22]. Therefore, a multicriteria decision analysis method should be applied to make an optimal decision between the switching losses and power fluctuation. The technique for Order of Preference by Similarity to Ideal Solution (TOPSIS) is one of the multicriteria decision analysis models proposed by Huang and Yun in 1981 [23]. It establishes the optimum alternative by calculating the distances between each alternative and the positive and negative-ideal solutions. It is based on an aggregating function of the expert evaluation ratings [23], [24]. The optimal solution would be the farthest from the negative-ideal solution and closest to the positive-ideal answer.

This paper will introduce a hybrid TOPSIS and FCS-MPC-based MPPT method for the PEMFC system. The techniques proposed in this paper include the TOPSIS algorithm, which can keep the maximum output power while minimizing the switching frequency. It will first predict and compute the PEMFC output voltage, current, and power for ON and OFF switching states at the next sampling step. Then, the switching frequency reduction process will be carried out by the TOPSIS algorithm by comparing the output power with its switching state. Lastly, the most suitable switching state with maximum output power and minimum switching frequency will be determined. The newly developed predictive-TOPSIS-based MPPT method may place a premium on fast MPP tracking and accuracy.

2. RESEARCH METHOD

A hybric predictive-TOPSIS-based MPPT method is proposed for a PEMFC system. This paper will simulate the proposed MPPT method in MATLAB/Simulink environment. First, a PEMFC mathematical model constructed as a PEMFC will represent the operating condition. To maintain the PEMFC output power at MPP, a model of a DC–DC converter is subsequently constructed to control the PEMFC output voltage. An FCS-MPC-based MPPT technique is developed to identify the switching states of the DC–DC power converter with higher output power. A similar predictive MPPT controller was presented by Fam et al. [25]. However, the research done in Fam et al. [25] excludes the switching frequency reduction control. It fully emphasizes on the MPPT without considering the switching frequency. This research includes the switching frequency reduction while maximizing the output power by accommodating the FCS-MPC algorithm with TOPSIS algorithm. Applying TOPSIS analysis sought to produce a multiobjective controller and make an optimum decision between the maximum power and the switching frequency. The final stage is to evaluate the proposed predictive-TOPSIS-based MPPT technique by changing the operating parameters of the PEMFC.

2.1. PEMFC Mathematical Model

This entire section is dedicated to a crucial study, an accurate PEMFC mathematical model. The output power curve of PEMFC is nonlinear. A review of the research revealed that the output power characteristic could be significantly influenced by the membrane water content, cell temperature, and partial pressure of hydrogen and oxygen [14], [25]. Meanwhile, whenever the PEMFC directly supplies power to a resistive load, its output power will also be affected.

The mathematical model starts with the fundamentals of the thermodynamic energy from the FC. It is the enthalpy of formation, ΔH, formed from the electrochemical reactions [26]. There are two thermal energies included in this reaction. The first thermal energy is the Gibbs free energy, ΔG. The equation for Gibbs free energy is written as [11]:

$$\Delta G = \Delta G° - RT\left(\ln P_{H_2} + \frac{1}{2}\ln P_{O_2}\right) \tag{1}$$

For standard conditions, Gibbs free energy, $\Delta G° = -237.170 \, kJ \, mol^{-1}$ [26], gas constant, $R = 8.3143 \, J \, (mol \, °K)^{-1}$ and Faraday constant, $F = 96485 \, C$. T is the operating temperature in Kelvin (K). The unit for partial pressure of hydrogen, P_{H_2} and oxygen, P_{O_2} are atmospheric pressure (atm). This equation shows that the energy from the FC highly depends on the partial pressures of the reactance gases.

The second thermal energy is the specific entropy, ΔS. Its mathematical function with the temperature that indicates the electric potential provided by the FC is shown in (2) [26]:

$$\Delta E = \frac{\Delta S}{nF}(T - T_{ref}) \tag{2}$$

Specific entropy, $\Delta S = -164\,J\,mol^{-1}\,°K^{-1}$, number of electrons released, $n = 2$, due two electrons released from the anode, and standard temperature, $T_{ref} = 298.15\,°K$. By merging (1) and (2), the Nernst equation can be derived, and it represents the initial electric potential from the FC.

$$E_{Nernst} = -\frac{\Delta G°}{nF} + \frac{\Delta S}{nF}(T - T_{ref}) + \frac{RT}{nF}\ln P_{H_2}P_{O_2}^{0.5} \tag{3}$$

By substituting all of the constant values, the simplified Nernst equation is:

$$E_{Nernst} = 1.229 - 8.5 \times 10^{-4}(T - 298.15) + 4.308 \times 10^{-5}T\ln P_{H_2}P_{O_2}^{0.5} \tag{4}$$

For hydrogen partial pressure, P_{H_2} and oxygen partial pressure, P_{O_2} the equations are defined in the time domain as shown in (5) and (6) [14]:

$$P_{H_2}(t) = \frac{1}{k_{H_2}}\left(2k_r I_{FC}e^{\left(\frac{-t}{\tau_{H_2}}\right)} + q_{H_2}^{in} - 2k_r I_{FC}\right) \tag{5}$$

$$P_{O_2}(t) = \frac{1}{k_{O_2}}\left(k_r I_{FC}e^{\left(\frac{-t}{\tau_{O_2}}\right)} + q_{O_2}^{in} - k_r I_{FC}\right) \tag{6}$$

The unit for operating time, t, is in second (s). The valve molar constants of the hydrogen, k_{H_2} and the valve molar constants of the oxygen, k_{O_2} are in unit ($kmol\,atm^{-1}\,s^{-1}$). The equation of modeling constant with unit ($kmol\,s^{-1}\,A^{-1}$) is given as $k_r = \frac{N}{4F}$. The time constant of the hydrogen, τ_{H_2} and time constant of the oxygen, τ_{O_2} are also in second (s). The molar flow of hydrogen, q_{H_2} and the molar flow of oxygen, q_{O_2} are in unit ($kmol^{-1}\,s^{-1}$).

The theoretical reversible thermodynamic potential in (V) can be calculated using the Nernst equation [14]. It also reflects the FC open-circuit voltage. However, the FC will experience a voltage drop: activation overvoltage, ohmic overvoltage and concentration overvoltage. Consequently, the FC output voltage with a single cell is described as:

$$V_{cell} = E_{nerst} - V_{act} - V_{ohm} - V_{conc} \tag{7}$$

where FC output stack voltage, V_{cell}, activation overvoltage, V_{act}, ohmic overvoltage, V_{ohm}, and concentration overvoltage, V_{con} are in unit voltage (V).

The activation overvoltage defined by the Tafel equation represents the voltage drop based on the reaction rate of the electrodes [14]. The equation of the activation overvoltage is shown in (8):

$$V_{act} = \xi_1 + \xi_2 T + \xi_3 T\ln C_{O_2} + \xi_4 T\ln I_{FC} \tag{8}$$

where ξ_1, ξ_2, ξ_3, and ξ_4 are the coefficients of the FC model. The FC output current, I_{FC} is in ampere (A), and the concentration of the dissolved oxygen, C_{O_2} is in unit ($mol\,cm^{-3}$). The equation for the dissolved oxygen concentration is defined as:

$$C_{O_2} = \frac{P_{O_2}}{(5.08 \times 10^6)e^{\frac{-498}{T}}} \tag{9}$$

Ohmic overvoltage is the term for the voltage drop based on the resistance of the proton membrane during the transfer of proton and electron. It resembles Ohm's law [26]:

$$V_{ohm} = I_{FC}(R_m) \tag{10}$$

and the electrode resistance, R_m can be defined as:

$$R_m = \frac{r_m t_m}{A} \tag{11}$$

From (11), the length of the electrolyte, t_m is in centimeter (cm) and the area of the electrolyte, A is in unit (cm^2). The electrolyte resistivity, r_m is the resistivity with unit ($\Omega\ cm$) which can be expressed as [14]:

$$r_m = 181.6 \frac{1 + 0.03 \left(\frac{I_{FC}}{A}\right) + 0.0062 \left(\frac{T}{303}\right)^2 \left(\frac{I_{FC}}{A}\right)^{2.5}}{\lambda_m - 0.634 - 3 \left(\frac{I_{FC}}{A}\right) e^{4.18\left(\frac{T-303}{T}\right)}} \tag{12}$$

The membrane water content, λ_m is from 0 to 14, indicating the relative humidity between 0% and 100%. This value may be increased up to 20 under ideal conditions [5] and it can reach 23 under supersaturated conditions [27].

Concentration overvoltage is caused by a decrease in gas concentration. Whenever the reactant concentration gradient is used during the process, a voltage drop occurs. This equation is shown in (13) [14]:

$$V_{con} = -\frac{RT}{nF} \ln\left(1 - \frac{I_{FC}}{i_L A}\right) \tag{13}$$

where the limiting current density, i_L is in unit ($A\ cm^{-2}$).

By computing (4)–(13), the FC output voltage of a single cell can be calculated. However, a single cell's voltage seems to be rather low. To increase the output voltage, multiple cells must be coupled with a bipolar plate. For a PEMFC with a stack of cells, the FC output voltage highly depends on the number of cells, N. The equation of FC output power with unit volt (V) is defined as:

$$V_{FC} = N V_{cell} \tag{14}$$

Then, the output power (W) can also be computed as:

$$P_{FC} = V_{FC} I_{FC} \tag{15}$$

2.2. DC–DC Boost Converter

This section focuses on the power electronics used in the proposed MPPT technique. Power electronics are required to control the PEMFC output voltage reaching the maximum power voltage so that the PEMFC operates at MPP [1]. In this paper, the PEMFC output voltage is controlled via a conventional DC–DC boost converter. It has the characteristic of stepping up the electrical DC voltage to a high level [10]. There is a switch inside the boost converter, which switches ON and OFF, and the one controlling the switching duration for one cycle is the duty cycle, D. It regulates the output voltage based on the input voltage by adjusting the duty cycle. A conventional DC–DC boost converter needs an inductor, a switch, a diode, and a capacitor as the primary components, and its circuit diagram is shown in Figure 2.
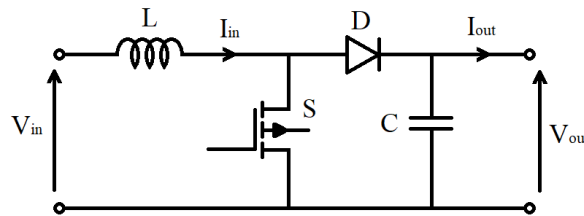

Figure 2. DC–DC Boost Converter

The equation of a DC–DC boost converter is defined as [10]:

$$V_{out} = \frac{V_{in}}{1 - D} \tag{16}$$

For an ideal converter, no power consumption is dissipated to the diode and switch. Therefore, following Kirchhoff's voltage law, the equation when the switch is turned OFF and ON can be expressed as:

$$S = 0, V_{in}(t) = L\frac{dI_{in}(t)}{dt} + V_{out}(t) \tag{17}$$

$$S = 1, V_{in}(t) = L\frac{dI_{in}(t)}{dt} \tag{18}$$

where t is the time taken after the PEMFC operation is started.

2.3. Predictive MPPT Technique

Specifically, this study sought the MPPT control application in a PEMFC system. The existing MPPT methods listed in the literature review can be applied to the PEMFC system. However, most of the methods have their drawback when tracking the MPP. This study proposes a simple way to address this issue using an FCS-MPC technique on MPPT, specialized for PEMFC. The method attempts to solve the problem following

a two-step process. First, it reads PEMFC parameters affecting the polarization curves and gives different MPPs. Second, these parameters are used to compute the MPP of the PEMFC.

The MPPT algorithm will be combined with the equation of the DC–DC boost converter. When it is connected to the PEMFC, the PEMFC voltage becomes the input voltage of the boost converter. Therefore, (17) and (18) can be simplified as:

$$S = 0, V_{FC}(t) = L\frac{dI_{FC}(t)}{dt} + V_{out}(t) \tag{19}$$

$$S = 1, V_{FC}(t) = L\frac{dI_{FC}(t)}{dt} \tag{20}$$

When FCS-MPC is applied to the MPPT, it can predict the behavior of the PEMFC output current of a system in future steps. Therefore, a discrete-time model mathematical equation is required to predict the future behavior in every sampling step. The FCS-MPC MPPT algorithm uses the same concepts to predict the PEMFC output current, and the discrete time (21) and (22) are derived as:

$$S = 0, I_{FC}(k + 1) = \frac{T_s}{L}\big(V_{FC}(k) - V_{out}(k)\big) + I_{FC}(k) \tag{21}$$

$$S = 1, I_{FC}(k + 1) = \frac{T_s V_{FC}(k)}{L} + I_{FC}(k) \tag{22}$$

where the discrete sampling steps is written as k and the sampling time is written as T_s. After the output current is predicted, PEMFC output voltage and power can also be predicted using (4) to (15). Using this algorithm can define the next PEMFC output power for ON and OFF switching states.

2.4. TOPSIS Algorithm

Besides the maximum output power, minimizing the switching frequency is also important to reduce the switching loss. In this study, the TOPSIS algorithm will take part in selecting the ideal switching state. It will determine a better selection for the multicriteria decision between the output power and the switching frequency. The first step of TOPSIS is constructing a 2×2 decision matrix comprising predicted output power as the two criteria and switching states as the two alternatives. The 2×2 decision matrix is shown in Figure 3.

Switching State	Output Power	Switching Change
OFF	x_{11}	x_{12}
ON	x_{21}	x_{22}

Figure 3. TOPSIS Decision Matrix

A specific normalization technique will be chosen to bring all the criteria to the same scale. Normalization aims to convert the matrix to become dimensionless, so that various criteria can be compared. In this work, the element of the decision matrix is normalized using (23):

$$r_{ij} = \frac{x_{ij}}{\sqrt{\Sigma x_{ij}^2}} \tag{23}$$

The concept of the weighting factor w_j will be introduced to set priority to each criterion so that a good trade-off between each criterion will be obtained. The matrix is a product of normalized decision score with its associated weight as (24):

$$v_{ij} = w_j r_{ij} \tag{24}$$

Where w_j is the weighting factor of each criterion. At this stage, the decision matrix becomes the weighted normalized decision matrix. In this paper, the weighting factor for the PEMFC output power and the switching are 99.9995 and 0.0005, respectively. This is because the output power is more important than the switching changes.

Next, the algorithm will identify the positive-ideal solutions (PIS) and negative-ideal solutions (NIS), covering all the beneficial criteria and the nonbeneficial criteria, respectively. In this research, the output power generation is a beneficial criterion and switching changes is a nonbeneficial criterion. For PIS, the highest output power, v_1^+ and the low switching change, v_2^+ will be selected. Contrary, the lowest output power, v_1^- and the high switching change, v_2^- will be selected as the NIS.

The Euclidean distance between PIS, S_i^+ and NIS, S_i^- to each switching state will be performed to evaluate how much they deviate from NIS and PIS. The equations are shown in (25) and (26) below.

$$S_i^+ = \sqrt{\sum_{i=1}^{m}\left(v_i^+ - v_{ij}\right)^2} \tag{25}$$

$$S_i^- = \sqrt{\sum_{i=1}^{m}\left(v_i^- - v_{ij}\right)^2} \tag{26}$$

The last step of TOPSIS is to calculate the relative closeness of each alternative to the ideal solution. The equation is given by:

$$C_i = \frac{S_i^-}{S_i^- + S_i^+} \tag{27}$$

After the relative closeness index is determined, the TOPSIS algorithm will select the solution with the higher relative closeness index. Therefore, the next switching state can be determined. Finally, the algorithm controls the switching state inside the boost converter and manages the PEMFC output voltage at MPP. The PEMFC output voltage will be maintained at a level where the PEMFC output power is at maximum. The process of the predictive-TOPSIS-based MPPT is shown in the flowchart below.
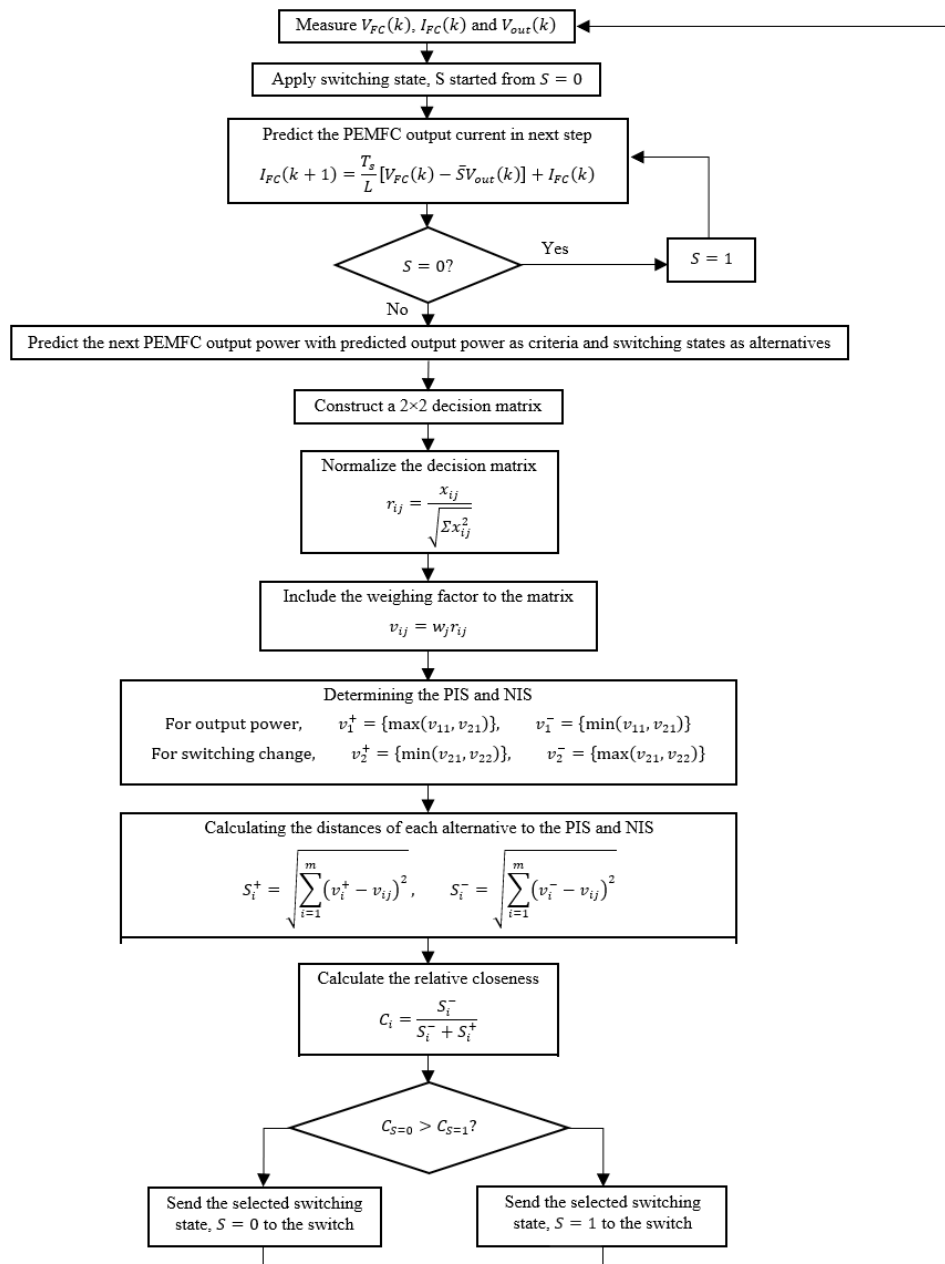

Figure 4. Predictive-TOPSIS-based MPPT Method Flow Chart

3. RESULTS AND DISCUSSION

This section shows the results performed using commercial software from MATLAB/Simulink. By default, the PEMFC parameters are set to be constant, as shown in Table 2.

Table 2. PEMFC Parameters

Parameter	Symbol & Unit	Value
Temperature	$T\ (K)$	343
Membrane water content	λ_m	14
Number of cells	N	35
Active area	$A\ (cm^2)$	232
Hydrogen valve molar constant	$k_{H_2}\ (kmol\ atm^{-1}\ s^{-1})$	4.22×10^{-5}
Oxygen valve molar constant	$k_{O_2}\ (kmol\ atm^{-1}\ s^{-1})$	2.11×10^{-5}
Hydrogen time constant	$\tau_{H_2}\ (s)$	3.37
Oxygen time constant	$\tau_{O_2}\ (s)$	6.74
Hydrogen input flow	$q_{H_2}\ (kmol\ s^{-1})$	1×10^{-4}
Oxygen input flow	$q_{O_2}\ (kmol\ s^{-1})$	5×10^{-5}
Membrane thickness	$t_m\ (cm)$	0.0178
Coefficient 1	ξ_1	0.944
Coefficient 2	ξ_2	−0.00354
Coefficient 3	ξ_3	$−7.8 \times 10^{-8}$
Coefficient 4	ξ_4	1.96×10^{-4}
Limiting current density	$i_L\ (A\ cm^{-2})$	2
Resistance	$R_L\ (\Omega)$	10

Three simulations have been done. For the first scenario, the proposed predictive-TOPSIS-based MPPT implemented to the PEMFC is simulated using the precise values in Table 2. For the second scenario, the simulation is repeated with various membrane water content and operating temperatures to verify the reliability of the predictive-TOPSIS-based MPPT. The last scenario is to validate the predictive-TOPSIS-based MPPT approach with the different resistance at the load side. All the results are compared with the predictive MPPT control technique in Fam et al. [25].

3.1. Simulation with Constant PEMFC Parameters

A schematic of the theoretical P–I curve using the parameters in Table 2 (Figure 5). The curve shows the maximum PEMFC output power at 8630 W, and the current is at 352.8 A.
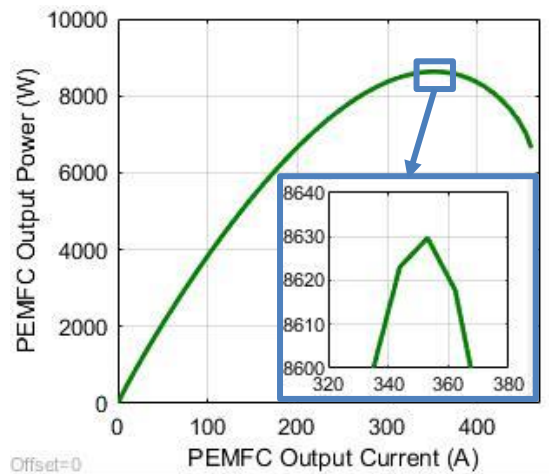

Figure 5. PEMFC P–I Characteristic (T = 343 K, λm = 14)

Figure 6a–6c show schematically the simulation PEMFC output voltage, PEMFC output current, and PEMFC output power obtained. Figure 6c shows that the PEMFC output power can achieve 8629 W within 0.02 s when the operation is started. Concurrently, the output voltage and current achieve 24.5 V and 352 A, respectively. By carefully examining the data, the predictive-TOPSIS-based MPPT algorithm was found to control the output voltage at MPP. However, there is a 43% voltage undershoot, 31% of current overshoot, and 25% of power undershoot before achieving the maximum power. Also, the PEMFC output has 5.7 % of voltage ripple, 6% of current ripple, and 0.15% of power ripple.
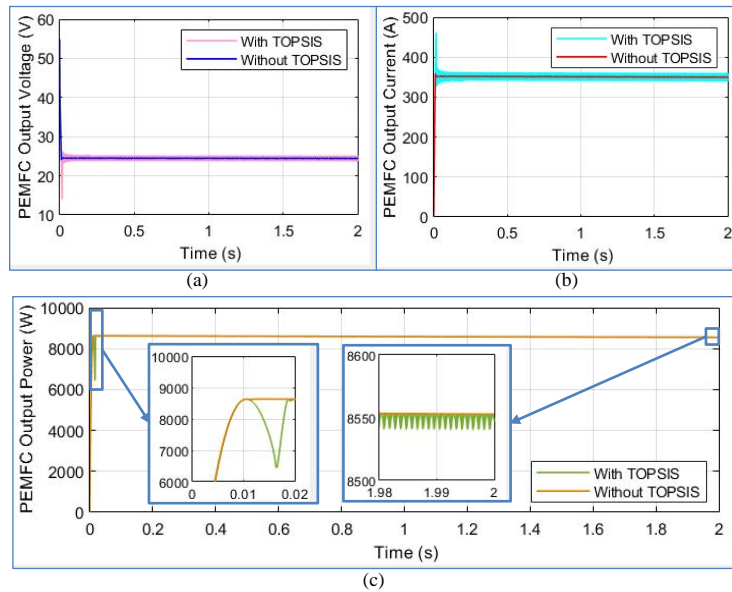
Figure 6. Simulation Results for constant PEMFC Parameters,
a), PEMFC Output Voltage, b) PEMFC Output Current, c) PEMFC Output Power

From Figure 6(c), the PEMFC output power is decreased from 8629 to 8550 W within 2 s. This phenomenon can be simply interpreted, based on the partial pressures of reactance gases being reduced over time during the process. This relates to the equation of partial pressure of reactant gases that was previously explored in (5). Initially, the hydrogen partial pressure is $q_{H_2}^{in}\big/k_{H_2}$. It reduced by $\left(2k_r I_{FC} - 2k_r I_{FC} e^{\left(-\frac{t}{\tau_{H_2}}\right)}\right)\big/k_{H_2}$ with time when the PEMFC started to operate. The final partial pressure of hydrogen is $\left(q_{H_2}^{in} - 2k_r I_{FC}\right)\big/k_{H_2}$ after a long-time operation process. The same appearance has occurred in partial pressure of oxygen, as explored in (6). This phenomenon has also been observed in [14] with the plotted graph.

From the results, the proposed predictive-TOPSIS-based MPPT technique appears to tally with our expectations of fast MPP tracking and high accuracy. However, the predictive TOPSIS-based MPPT controller has higher output voltage, current, and power than the predictive MPPT method without frequency reduction. This is because the proposed TOPSIS-based MPPT consider the switching frequency and reduce it to a lower scale. It means that the proposed predictive TOPSIS-based MPPT controller minimizes the switching frequency while maintaining the maximum output current simultaneously. Although the output power quality is not as good as the predictive MPPT method presented in Fam et al. [25], its power ripple is can still be deemed as low fluctuation. By comparison, predictive-based TOPSIS MPPT method can reduce the switching frequency from 22000 to 900 Hz. According to Onederra et al. [18], the switching loss can be minimized if the switching frequency can be decreased. The most significant observation of this study is that the switching frequency is reduced to a low scale, suitable for IGBT and can withstand the high current and high power. Figure 7 compares the switching state determined by the predictive algorithm with TOPSIS and without TOPSIS.
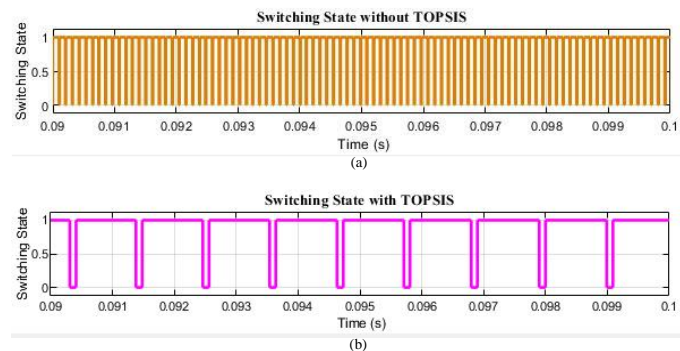

Figure 7. Switching State Selected by MPPT Controller,
a)   Without TOPSIS, b) With TOPSIS

The results were directly compared with the previously reported findings by Ahmadi et al. [14]. In Ahmadi et al. [14], the PEMFC model used is exactly same as the mathematical model presented in this paper. The simulation results include the particle swarm optimization with proportional-integral-derivative controller (PSO-PID), P&O, and sliding mode (SM) methods. The predictive-TOPSIS-based MPPT approach has an extremely short tracking time and high accuracy when the results are compared with the other MPPT methods. A summary of the comparison results is given in Table 3.

Table 3. MPPT Techniques Comparison

MPPT Technique	MPPT Accuracy	Settling Time	Power Ripple	Switching Frequency
Predictive-TOPSIS-based MPPT (proposed)	99.11%	0.019 s	0.15%	900Hz
Predictive MPPT [25]	99.11%	0.012 s	0.002%	22000Hz
PSO–PID [14]	98.63%	0.070 s	-	-
SMC [14]	98.30%	0.100 s	0.7%	-
P&O [14]	97.81%	0.900 s	1.7%	-

Results illustrated in Table 3 show that the PSO–PID approach can obtain the maximum power of the FC within 0.07 s. However, the suggested predictive-TOPSIS-based MPPT method only require 0.019 s to achieve 99.11% of the theoretical maximum power. The settling time is around five times shorter than the PSO–PID approach. It performed with a quick MPP tracking so that it can reach the PEMFC maximum power faster. In addition, the tracking accuracy of the suggested predictive-TOPSIS-based MPPT approach is the best among the MPPT technique in Table 3, with 99.11% theoretical maximum power. It can be concluded that the proposed MPPT method has an outstanding performance in terms of tracking accuracy and settling time. For power quality, the predictive-TOPSIS-based MPPT method shows a lower power ripple than SMC and P&O methods. However, the power ripple for PSO–PID method cannot be observed so the comparison is not available. Although the switching frequency is inaccessible in Ahmadi et al. [14], it is not significant to compare the switching frequency. This is because the switching frequency for the proposed technique is low for the IGBT to operate.

3.2. Simulation with Variable PEMFC Parameters

For the second simulation, the performance of the proposed MPPT technique was tested under various operating temperatures and membrane water content. To compare with other published results, the simulation is divided into two parts. First, the simulation is done by increasing the operating temperature from 323 to 363 K and then back to 323 K under constant membrane water content of 14. Then, the simulation is repeated by increasing the membrane water content from 12 to 16 and then back to 12 under constant operating temperature of 343 K. The changes in membrane water content and operating temperature over time are presented in Figure 8a and 8b.

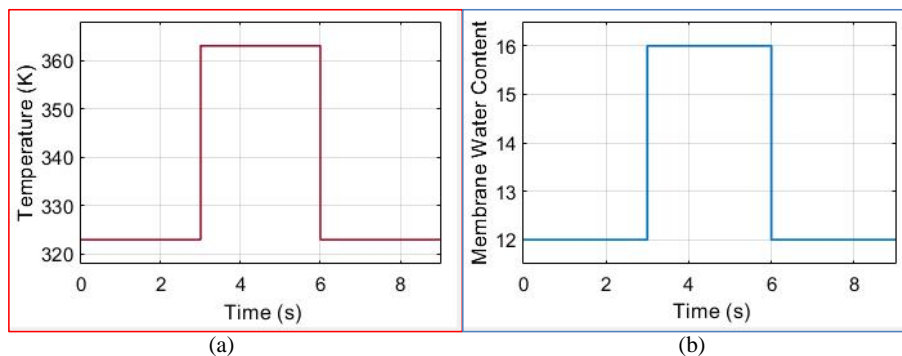
(a)   (b)

Figure 8. Fast Variation of PEMFC Parameters with Time,
a) Operating Temperature, b) Membrane Water Content

Figure 9a and 9b compare the simulation results of the predictive MPPT method with TOPSIS and without TOPSIS. It is found that both the methods can track the MPP. The settling time for predictive-TOPSIS-based MPPT is slightly longer than the predictive MPPT method. However, predictive-TOPSIS-based MPPT has outstanding control on lowering the switching frequency. When the FC parameter changes, both methods undergo similar voltage overshoot, voltage undershoot, and power undershoot. The transient time is extremely short, within 3 ms. It means that tracking the new MPP during the fast variation of parameters is extremely fast.
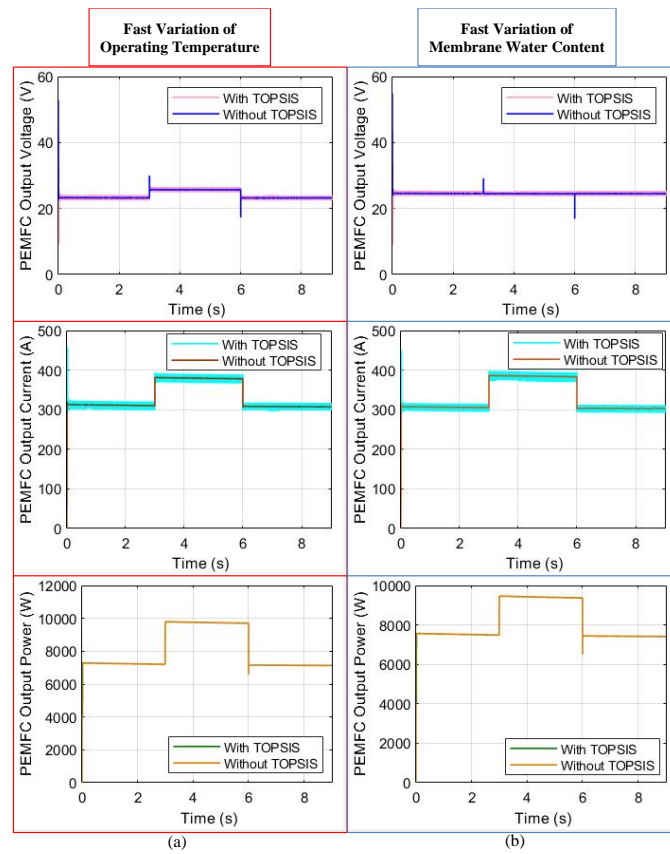
Figure 9. Simulation Results for Fast Variation of PEMFC Parameters,
a) Fast Variation of Operating Temperature, b) Fast Variation of Membrane Water Content

The obtained results are compared with the theoretical MPP and other published results presented in Ahmadi et al. [14] for all operating conditions. The comparison is tabulated in Table 4.

Table 4. Comparison of Simulation Results

Performance Comparison	Parameters		Theoretical	Predictive TOPSIS-based MPPT (proposed)	Predictive MPPT [25]	PSO–PID [14]	SMC [14]	P&O [14]
	T (K)	λ_m						
Maximum Power	323	14	7287 W	7157 W (98.2%)	7161 W (98.3%)	7136 W (97.9%)	7106 W (97.5%)	7060 W (96.9%)
	363	14	9940 W	9700 W (97.6%)	9706 W (97.6%)	9689 W (97.5%)	9666 W (97.2%)	9613 W (96.7%)
	343	12	7571 W	7410 W (97.9%)	7416 W (98.0%)	7408 W (97.8%)	7385 W (97.5%)	7329 W (96.8%)
	343	16	9601 W	9366 W (97.6%)	9373 W (97.6%)	9363 W (97.5%)	9339 W (97.3%)	9293 W (96.8%)
Transient Time (s)	323	14	-	0.0002 s	0.00025 s	-	-	0.1 s
	363	14	-	0.002 s	0.0025 s	-	-	0.3 s
	343	12	-	0.0003 s	0.0003 s	-	-	0.1 s
	343	16	-	0.003 s	0.003 s	-	-	0.4 s
Power Ripple	323	14	-	11 W (0.15%)	0.20 W (0.0028%)	-	50 W (0.70%)	130 W (1.84%)
	363	14	-	16 W (0.16%)	0.25 W (0.0026%)	-	40 W (0.41%)	140 W (1.46%)
	343	12	-	15 W (0.20%)	0.2 W (0.0027%)	-	60 W (0.81%)	150 W (2.05%)
	343	16	-	12 W (0.13%)	0.2 W (0.0021%)	-	50 W (0.54%)	130 W (1.40%)
Power Undershoot	323	14	-	5.97%	8.32%	7.51%	9.94%	9.35%
	343	12	-	12.5%	12.7%	10.9%	12.0%	11.3%
Switching Frequency	323	14	-	11000 Hz	80000 Hz	-	-	-
	363	14	-	10000 Hz	80000 Hz	-	-	-
	343	12	-	11000 Hz	90000 Hz	-	-	-
	343	16	-	10000 Hz	70000 Hz	-	-	-

This finding is expected since the predictive-TOPSIS-based MPPT technique can track the MPP in various parameters. For each parameter setting, the proposed predictive-TOPSIS-based MPPT technique can track the MPP with a higher percentage than with PSO–PID, P&O, and SM methods. However, some performances are inaccessible, and no comparison can be made. Although its output power performance is slightly worse than the predictive MPPT method, its switching frequency is far lower than the predictive MPPT method without the switching frequency reduction technique. In addition, this simulation primarily found that it is robust to parameter changes since it can track the next MPP quickly.

3.3. Simulation with Variable Resistance

This simulation validates the proposed MPPT technique when the resistance at the load side varies rapidly. For this simulation, the resistance was set to 12 Ω and increased 2 Ω for every 0.4 s until it reached 20 Ω. The simulation PEMFC output power is shown in Figure 10.
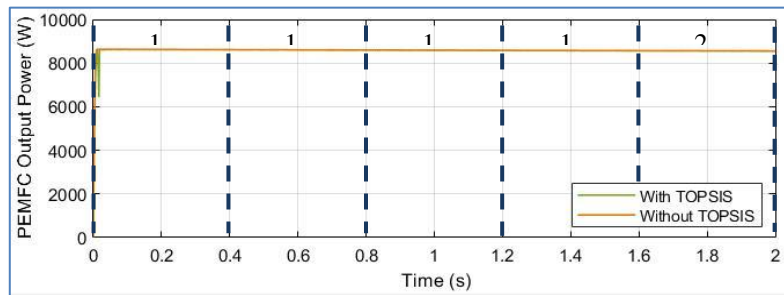
Figure 10. PEMFC Output Power with Fast Variation of Load Resistance

The above figure illustrates the fact that the simulation result is as good as Figure 6c. The predictive-TOPSIS-based MPPT and the predictive MPPT approach show similar performance. The simulation result shows no power transient when the load resistance is changed. It is proven that the predictive-TOPSIS-based MPPT approach is robust to resistance variations at the load side. The simulation result can be compared with the other published results in [28]. Although the simulation setup is slightly different from the model presented in this paper, it shows a similar P–I characteristic curve of PEMFC introduced in this paper. The journal reported the results of changing the load resistance affecting the PEMFC output power generation. From the result presented in [28], the dynamic response of PEMFC output power occurs as a power transient. Therefore, it can be deduced that the proposed MPPT technique is highly robust to load resistance changes.

The voltage, current, and power for the load side are shown in Figure 11a–11c, respectively. The resistor maintains the consumption of electrical power lower than the maximum power generated by the PEMFC even when the resistance changes. This is because some power is consumed by the DC–DC converter. However, the voltage and current change during the variation of the resistance. It has strong theoretical foundations in Ohm's Law and the formula of power. The equation of Ohm's Law and the formula of power are shown in (28) and (29) below.

$$V = IR \qquad (28)$$
$$P = VI \qquad (29)$$

These two equations express the relationship between power, voltage, and current.

$$P = \frac{V^2}{R} \qquad (30)$$
$$P = I^2 R \qquad (31)$$

When the power is maintained, the voltage and current will be varied if the resistance is changed.

From Figure 11a and 11b, the voltage is increased while the output current is decreased. However, Figure 11c shows the load power was maintained at 8400 W with five power transients. The summary of the load voltage, load current, and load power are presented in Table 5. These power transient states occur during the rapid variation of the resistance. This is because there was a current undershoot when the resistance changed suddenly. When resistance is changed rapidly, the voltage requires 0.2 s to reach the regulated voltage. The voltage does not rise immediately due to the capacitor, which works against voltage changes, causing the voltage rise to become slower. This will also lead the current to undershoot and causes the power to transient.
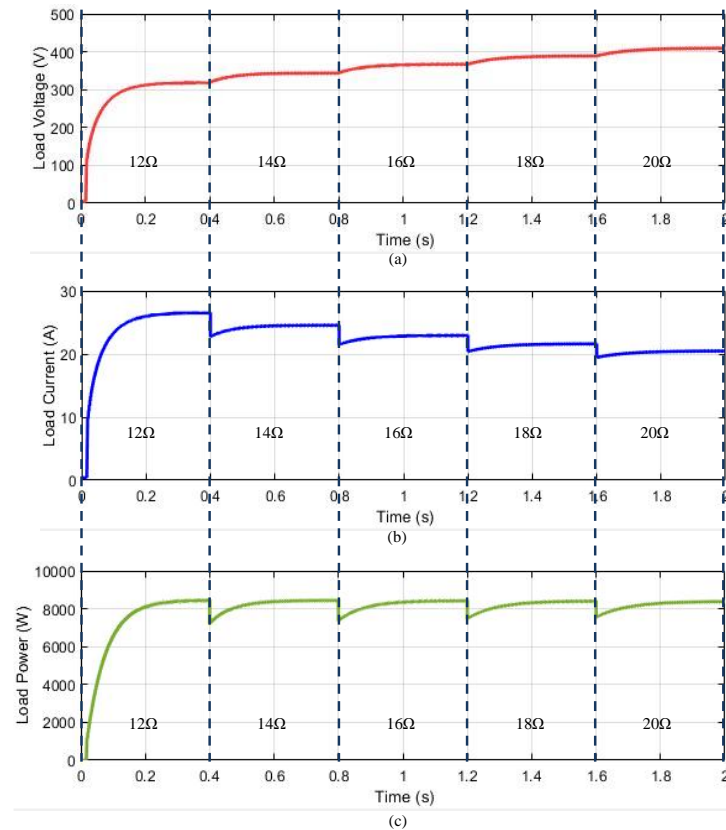
Figure 11. Simulation Results for Fast Variation of Resistance at the Load Side,
(a) Load Voltage, (b) Load Current, (c) Load Power

Table 5. Voltage, Current, and Power of Resistor at the Load Side

Resistance (Ω)	Voltage (V)	Current (A)	Power (W)
12	318	26.5	8437
14	344	24.5	8428
16	367	22.9	8404
18	389	21.6	8402
20	409	20.4	8344

4. CONCLUSION

A predictive-TOPSIS-based MPPT technique specialized for PEMFC is developed. The outcome of various experiments concludes that the FCS-MPC-based MPPT approach can predict the next PEMFC output power based on the current step. After that, TOPSIS algorithm compares the predicted maximum power and the present switching state to decide the next switching state. It helps to minimize the switching frequency while keeping the PEMFC output power at maximum. As a result, the predictive-TOPSIS-based MPPT method reduces the switching frequency from 22000 to 900 Hz. It also shows an excellent performance in fast MPP tracking and accuracy when compared with other MPPT approaches. The most significant observation of this study is that the suggested predictive-TOPSIS-based MPPT method has the shortest tracking time of MPP, within 0.019 s, and the highest accuracy up to 99.11%. For the fast variation of PEMFC parameters, the predictive MPPT technique can establish the output power to the new MPP within 3 ms, minimizing power loss. In addition, the proposed MPPT method can keep the PEMFC output power at MPP even when the load resistance is changed. Overall, the technique produces excellent results for tracking time of the MPP, high accuracy, and robustness to parameter changes. Although the results presented in this paper are only simulations, they highly reflect real-life PEMFC. Therefore, developing the proposed MPPT technique by simulation is persuasive. The experimental work will be carried out for future work.

REFERENCES

[1]   [1] N. Karami, L. El Khoury, G. Khoury, and N. Moubayed, "Comparative study between P&O and incremental conductance for fuel cell MPPT," *2014 Int. Conf. Renew. Energies Dev. Countries, REDEC 2014*, no. 2, pp. 17–22, 2014, doi: 10.1109/REDEC.2014.7038524.

[2]   [2] V. Boscaino, R. Miceli, and G. Capponi, "MATLAB-based simulator of a 5 kW fuel cell for power electronics

design," *Int. J. Hydrogen Energy*, vol. 38, no. 19, pp. 7924–7934, 2013, doi: 10.1016/j.ijhydene.2013.04.123.

[3]   [3] B. Gou, W. Ki Na, and B. Diong, *Fuel Cell Modeling, Control, and Applications*. Boca Raton, USA: Taylor and Francis, 2010.

[4]   [4] Z. dan Zhong, H. bo Huo, X. jian Zhu, G. yi Cao, and Y. Ren, "Adaptive maximum power point tracking control of fuel cell power plants," *J. Power Sources*, vol. 176, no. 1, pp. 259–269, 2008, doi: 10.1016/j.jpowsour.2007.10.080.

[5]   [5] J. Jiao and X. Cui, "Adaptive control of MPPT for fuel cell power system," *J. Converg. Inf. Technol.*, vol. 8, no. 4, pp. 362–371, 2013, doi: 10.4156/jcit.vol8.issue4.43.

[6]   [6] S. Abdi, K. Afshar, N. Bigdeli, and S. Ahmadi, "A novel approach for robust maximum power point tracking of PEM fuel cell generator using sliding mode control approach," *Int. J. Electrochem. Sci.*, vol. 7, no. 5, pp. 4192–4209, 2012.

[7]   [7] N. Naseri, S. El Hani, A. Aghmadi, K. El Harouri, M. S. Heyine, and H. Mediouni, "Proton exchange membrane fuel cell modelling and power control by P&O algorithm," *Proc. 2018 6th Int. Renew. Sustain. Energy Conf. IRSEC 2018*, pp. 1–5, 2018, doi: 10.1109/IRSEC.2018.8703002.

[8]   [8] S. Dharani and R. Seyezhai, "Development of simulator and MPPT algorithm for PEM fuel cell," *Commun. Appl. Electron.*, vol. 2, no. 7, pp. 36–41, 2015, doi: 10.5120/cae2015651774.

[9]   [9] M. Dargahi, M. Rezanejad, J. Rouhi, and M. Shakeri, "Maximum power point tracking for fuel cell in fuel cell/battery hybrid systems," *IEEE INMIC 2008 12th IEEE Int. Multitopic Conf. - Conf. Proc.*, no. 2, pp. 33–37, 2008, doi: 10.1109/INMIC.2008.4777703.

[10]   [10]   M. Derbeli, O. Barambones, M. Farhat, and L. Sbita, "Efficiency boosting for proton exchange membrane fuel cell power system using new MPPT method," *2019 10th Int. Renew. Energy Congr. IREC 2019*, no. Irec, pp. 1–4, 2019, doi: 10.1109/IREC.2019.8754587.

[11]   [11]   M. Derbeli, O. Barambones, and L. Sbita, "A robust maximum power point tracking control method for a PEM fuel cell power system," *Appl. Sci.*, vol. 8, no. 12, 2018, doi: 10.3390/app8122449.

[12]   [12]   D. N. Luta and A. K. Raji, "Fuzzy rule-based and particle swarm optimisation MPPT techniques for a fuel cell stack," *Energies*, vol. 12, no. 5, 2019, doi: 10.3390/en12050936.

[13]   [13]   S. Srinivasan, R. Tiwari, M. Krishnamoorthy, M. P. Lalitha, and K. K. Raj, "Neural network based MPPT control with reconfigured quadratic boost converter for fuel cell application," *Int. J. Hydrogen Energy*, vol. 46, no. 9, pp. 6709–6719, 2021, doi: 10.1016/j.ijhydene.2020.11.121.

[14]   [14]   S. Ahmadi, S. Abdi, and M. Kakavand, "Maximum power point tracking of a proton exchange membrane fuel cell system using PSO-PID controller," *Int. J. Hydrogen Energy*, vol. 42, no. 32, pp. 20430–20443, 2017, doi: 10.1016/j.ijhydene.2017.06.208.

[15]   [15]   M. Derbeli, A. Charaabi, O. Barambones, and C. Napole, "High-performance tracking for proton exchange membrane fuel cell system pemfc using model predictive control," *Mathematics*, vol. 9, no. 11, pp. 1–17, 2021, doi: 10.3390/math9111158.

[16]   [16]   J. Rodriguez and P. Cortes, *Predictive Control of Power Converters and Electrical Drives*. Chichester, UK: John Wiley & Sons, Ltd, 2012.

[17]   [17]   V. D. Tigadi, "Power losses in switch mode power converters," vol. 14, no. 3, pp. 43–48, 2019, doi: 10.9790/1676-1403014348.

[18]   [18]   O. Onederra, I. Kortabarria, I. M. De Alegria, J. Andreu, and J. I. Garate, "Three-phase VSI optimal switching loss reduction using variable switching frequency," *IEEE Trans. Power Electron.*, vol. 32, no. 8, pp. 6570–6576, 2017, doi: 10.1109/TPEL.2016.2616583.

[19]   [19]   Q. Cui, M. Liao, Z. Liao, and Z. Chen, "Frequency reduction-based model predictive direct power control with multi-cost function," vol. 143, no. Ammsa, pp. 241–245, 2018, doi: 10.2991/ammsa-18.2018.49.

[20]   [20]   T. J. L. Oliveira, L. M. A. Caseiro, A. M. S. Mendes, S. M. A. Cruz, and M. S. Perdigao, "Switching frequency reduction for efficiency optimization in two paralleled UPS systems," *Proc. - 2020 IEEE 14th Int. Conf. Compat. Power Electron. Power Eng. CPE-POWERENG 2020*, pp. 161–166, 2020, doi: 10.1109/CPE-POWERENG48600.2020.9161560.

[21]   [21]   V.-T. Dang, M.-G. Yang, C.-H. Jang, S. Lee, Y. Shim, and K.-H. Baek, "A highly efficient time-based MPPT circuit with extended power range and minimized tuning switching frequency," *IEEE Access*, vol. 10, no. May, pp. 64004–64017, 2022, doi: 10.1109/access.2022.3183280.

[22]   [22]   H. J. Lee, J. J. Jung, and S. K. Sul, "A switching frequency reduction and a mitigation of voltage fluctuation of modular multilevel converter for HVDC," *2014 IEEE Energy Convers. Congr. Expo. ECCE 2014*, pp. 483–490, 2014, doi: 10.1109/ECCE.2014.6953433.

[23]   [23]   G.-H. Tzeng and J.-J. Huang, *Multiple Attribute Decision Making Methods and Applications*. Taylor and Francis Group, LLC, 2011.

[24]   [24]   A. Jozaghi *et al.*, "A comparative study of the AHP and TOPSIS techniques for dam site selection using

GIS: A case study of Sistan and Baluchestan Province, Iran," *Geosci.*, vol. 8, no. 12, 2018, doi: 10.3390/geosciences8120494.

[25]   [25]   S. Chugh, C. Chaudhari, K. Sonkar, A. Sharma, G. S. Kapur, and S. S. V. Ramakumar, "Experimental and modelling studies of low temperature PEMFC performance," *Int. J. Hydrogen Energy*, vol. 45, no. 15, pp. 8866–8874, 2020, doi: 10.1016/j.ijhydene.2020.01.019.

[26]   [26]   E. W. Saeed and E. G. Warkozek, "Modeling and analysis of renewable PEM fuel cell system," *Energy Procedia*, vol. 74, pp. 87–101, 2015, doi: 10.1016/j.egypro.2015.07.527.

[27]   [27]   I. Soltani, "An intelligent, fast and robust maximum power point tracking for proton exchange membrane fuel cell," *World Appl. Program.*, vol. 3, no. July, pp. 264–281, 2013.

[28]   [28]   H. Rezk, "Performance of incremental resistance MPPT based proton exchange membrane fuel cell power system," *2016 18th Int. Middle-East Power Syst. Conf. MEPCON 2016 - Proc.*, pp. 199–205, 2017, doi: 10.1109/MEPCON.2016.7836891.

BIOGRAPHY OF AUTHORS

Jye Yun Fam was born in Sarawak, Malaysia in 1995. He received the B. Eng degree in electrical and electronics engineering from the Universiti Malaysia Sarawak (UNIMAS), Malaysia, in 2019. He is pursuing his PhD in maximum power point tracking for proton exchange membrane fuel cell with the Department of Electrical and Electronics Engineering, Universiti Malaysia Sarawak. His research work focuses on the energy efficiency of renewable energy.

Shen Yuong Wong (Senior Member, IEEE) is an associate professor in the Department of Electrical and Electronics Engineering, Xiamen University Malaysia. She received bachelor's and master's degrees (Hons.) in Electrical and Electronic Engineering from Universiti Tenaga National (National Energy University), Malaysia, and a Ph.D. degree in engineering from Universiti Tenaga National. Her research includes power system fault detection and diagnosis, extreme learning machine, classification, regression, and other applications of artificial intelligence. Dr. Wong is a professional engineer (PEng) registered to the Board of Engineers Malaysia (BEM), accredited under the Washington Accord. She serves as an editorial board member for several journals.
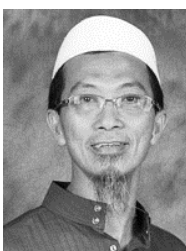
Mohammad Omar Abdullah received his BEng degree and MSc degree in Petroleum & Natural Gas Engineering from Universiti Teknologi Malaysia (UTM) in 1989 and 1991, respectively, and PhD degree from the University of Hertfordshire (UH), United Kingdom in 2002. He has been a Professor of Applied Energy and Environment at the Department of Chemical Engineering & Energy Sustainability (ChemES), Faculty of Engineering, Universiti Malaysia Sarawak (UNIMAS) since 2014. He is currently the founding Head of ChemES. His strength is indicated by his industrial-related research on applied energy & environment. He was appointed as a Senior Member of the Academy of Malaysian SMEs (SMAMS) in March 2009 during the IKS2009 Presentation and Exhibition, Putra World Trade Center, Kuala Lumpur. Professor Abdullah has been a registered member of IMechE and Charted Engineer (CEng) of United Kingdom since September 2004. He has also been a member of the American Society of Heating Refrigeration and Air-conditioning Engineers (ASHRAE) since August 2004. Also, he is the co-owner of OSYIHM Farm, a nonpesticide farm promoting clean hybrid energy use and supporting integrated healthy, sustainable farming.

Kasumawati Binti Lias (Member, IEEE) was born in Sarawak, Malaysia in 1981. She received the M.Eng. degree from Universiti Teknologi Malaysia, Malaysia in 2008 and Ph.D degree from Universiti Teknologi MARA, Malaysia in 2020. She is currently a lecturer of the Faculty of Engineering, Universiti Malaysia Sarawak, Malaysia. She has her research interest in biomedical engineering. Dr. Kasumawati is a registered professional engineer from the Board of Engineers, Malaysia.

Saad Mekhilef is an IEEE and IET Fellow. He is a distinguished professor at the School of Science, Computing and Engineering Technologies, Swinburne University of Technology, Melbourne, Australia, and an honorary professor at the Department of Electrical Engineering, University of Malaya. He authored and coauthored more than 500 publications in academic journals and proceedings and five books with more than 39,000 citations, and more than 70 Ph.D students graduated under his supervision. He serves as an editorial board member for many top journals, such as IEEE Transactions on Power Electronics, IEEE Open Journal of Industrial Electronics, IET Renewable Power Generation, Journal of Power Electronics, and International Journal of Circuit Theory and Applications. Professor Mekhilef has been listed by Thomson Reuters (Clarivate Analytics) as one of the Highly Cited (World's Top 1%) engineering researchers in the world in 2018, 2019, 2020, and 2021. He is actively involved in industrial consultancy for major corporations in the power electronics and renewable energy projects. His research interests include power conversion techniques, control of power converters, maximum power point tracking (MPPT), renewable energy, and energy efficiency.

Hazrul Bin Mohamed Basri (Member, IEEE) was born in Perak, Malaysia in 1984. He received the B.Eng. degree from Université de Technologie de Belfort Montbéliard, France in 2010 and Ph.D degree from Universiti Malaya, Malaysia in 2019. He is currently a senior lecturer in the Faculty of Engineering, Universiti Malaysia Sarawak, Malaysia. His research has been concerned with power electronics, renewable energy, and multiobjective optimization algorithm. Dr. Hazrul Mohamed Basri is a registered professional engineer from the Board of Engineers, Malaysia.